

A Framework for Planning LoRaWAN Networks

Matteo Cesana, Alessandro Redondi

Dipartimento di Elettronica, Informazione e Bioingegneria,
Politecnico di Milano,
Milano, Italy
{matteo.cesana, alessandroenrico.redondi}@polimi.it

Jorge Ortin

Centro Universitario de la Defensa,
50090 Zaragoza, Spain
jortin@unizar.es

Abstract—We set ourselves from the perspective of a LoRaWAN network operator and we introduce a mathematical programming framework to jointly optimize network layout and network configuration at design time. The proposed framework returns the most cost-effective network layout in terms of gateways position, gateways backhaul configuration and LoRaWAN physical parameters configuration under tight constraints of end node coverage, end-to-end message transmission latency and message extraction rate. Numerical results obtained on realistic network instances demonstrate that the proposed approach leads to network configuration with superior performance with respect to coverage-only classical design policies.

I. INTRODUCTION

Current cellular mobile networks were mainly designed for human-to-human and human-to-machine interactions targeting specific applications/services like telephony, SMS/MMS exchange, multimedia download and streaming; this is at odds with the vision and evolution of the Internet of Things (IoT) which requires connectivity also for unmanned devices. This *de facto* defines a new communication paradigm (and traffic) which involves little or no human interaction, and thus it is often referred to as Machine-To-Machine communications or Machine-Type Communications.

To this extent, the Third Generation Partnership Project (3GPP) launched several activities to improve classical cellular standards to effectively accommodate M2M communications including the Extended Coverage-GSM (EC-GSM), the LTE enhanced Machine Type Communication (LTE-M) and/or the Narrowband IoT (NB-IoT). However, the aforementioned technologies took a while for being standardized and did not reach yet the full maturity and diffusion. Such “delayed” time-to-market of IoT-compliant cellular standards opened up the way to IoT-specialized network operators selling IoT connectivity through long-range, low-power wireless technologies like SigFox [1], LoRaWAN [2], Weightless [3] and Ingenu [4].

We focus here on LoRaWAN, in which end devices use single-hop spread spectrum wireless transmission to reach one or multiple gateways which are then connected

with a backend server via standard IP-based technologies. The performance of LoRaWAN networks in terms of coverage, end-to-end latency and Data Extraction Rate (DER) depend jointly on the network layout (number/position of the gateways and type of backhauling technologies) and on the configuration of the physical layer parameters characterizing the wireless segment (spreading factor, protection coding rate, channel bandwidth, emitted power).

We set ourselves from the perspective of a LoRaWAN network operator with the specific target to optimize her network layout. Namely, we introduce a mathematical programming framework to jointly optimize network layout and network configuration at design time. The proposed framework returns the most cost-effective network layout in terms of gateways’ position, gateways’ backhaul configuration and LoRaWAN physical parameters configuration under tight constraints of end node coverage, end-to-end message transmission latency and message extraction rate. Differently than common approaches which consider only coverage in the network planning phase, the proposed model includes at design phase the configuration of the LoRaWAN radio parameters. Numerical results obtained on realistic network instances demonstrate that the proposed approach leads to network configurations with superior performance with respect to coverage-only classical design policies.

The manuscript is organized as follows: Section II reports on the related literature on LoRaWAN performance evaluation and design; in Section III, we overview the most distinctive features of LoRaWAN technology; Section IV describes the theoretical framework to optimize LoRaWAN network deployment, which is then used in Section V to design realistic networks running LoRaWAN. Section VI reports our concluding remarks with the indication of future research lines.

II. RELATED WORK

The research on LoRaWAN network is still in its infancy and so far mainly targeted the performance assessment of the physical and medium access control layers of the reference standard.

One of the first work reporting on the experimental evaluation of LoRa-based wireless link is [5] which mainly characterizes the coverage range of LoRa transmissions. Along the same lines, Petajarvi *et al.* evaluate in [6] and later in [7] the impact of different physical layer parameters onto the coverage range and robustness of LoRa links under different propagation environment. The work in [6] also proposes a path loss model to characterize LoRa propagation in the 868 MHz band. Similar experimental assessments of LoRa performance are proposed in [8] and [9]. Always with a practical approach the work in [10] “measures” the performance of LoRa in indoor environments with a focus on health-related applications, whereas [11] reports on experiments carried out with device-to-device LoRa transmissions.

System oriented performance evaluation is carried out in [12] which introduces a simulator of LoRaWAN named LoRaSim that is used to assess network-wide performance including transmission latency, and data extraction rate. LoRaSim is then leveraged by the same authors in [13] to analyze different strategies to mitigate the interference in multi-gateway LoRaWAN. LoRaSim is further extended by Pop *et al.* in [14] to include the support of bidirectional traffic. Simulation-based analysis of LoRaWANs is proposed also in [15] and [16], whereas Georgious *et al.* propose in [17] a theoretical framework based on stochastic geometry to derive the uplink outage probability in LoRaWAN.

Finally, the work in [18] and [19] propose non-standard add ons to improve LoRaWAN performance. Namely, Kim *et al.* describes a dynamic scheme to adjust the uplink LoRa data rate based on a predictor of the current network congestion level, whilst the work in [19] introduces and evaluates a non-standard coding scheme to improve LoRa transmission robustness.

The aforementioned literature on LoRaWAN mainly focuses on the performance evaluation of given LoRaWAN network layouts. Differently, in this work we address a network design problem and target the optimal design and configuration of LoRaWAN networks. To the best of our knowledge, ours is the first work providing an optimization framework to optimize LoRaWAN network layout and configuration at design time.

III. LORAWAN OVERVIEW

LoRaWAN is an open protocol wireless standard developed by the LoRa Alliance [2]. LoRaWAN reference architecture, shown in Figure 1.(b), includes the *end nodes* sensing and transmitting field data, *gateways* which collect the data from the end nodes and forward them to a *network server* where all the “intelligence” of the network is. The uplink segment from the end nodes to the gateways is association-less in the sense that end nodes are not associated to any specific gateway, but rather uplink-broadcast their messages which are received and forwarded upwards by any gateway in

range. The network server is then in charge of removing duplicates in the uplink messages, running the Medium Access Control logic and managing the LoRa RF parameters.

The communication in LoRaWAN networks happens according to the reference protocol stack reported in Figure 1.(a). LoRaWAN operates in the unlicensed radio spectrum in the Sub-GHz Industrial, Scientific and Medical (ISM) bands with region-specific carrier frequencies and PHY parameter configurations for Europe, North America, Asia, etc. The very heart of LoRaWAN physical layer is Long Range (LoRaTM), a proprietary spread spectrum modulation technique by Semtech based on a derivative of Chirp Spread Spectrum (CSS) which is robust to multipath fading, Doppler shift and narrowband interference, thus allowing to reach large link budget and processing gains.

The range and energy consumption of end devices mainly depend on four parameters at the physical layer: (i) the *channel bandwidth* (BW), chosen in the set [125kHz, 250kHz, 500kHz], defines the amplitude in the frequency domain of the used channel: higher bandwidth leads to higher throughput but to lower sensitivity (because of integration of additional noise); (ii) the *spreading factor* (SF) is a configuration parameter of the modulation techniques defined as the ratio between the symbol rate and chip rate. The number of chips per symbol is calculated as 2^{SF} , thus the SF tells “how much” the reference signal is spread in time; the higher the spreading factor the longer the transmission range but the lower the transmission rate; indeed, each increase in SF halves the transmission rate and, hence, doubles transmission duration and ultimately energy consumption; LoRa specifications define a discrete set of usable spreading factors from SF=7 to SF=12. (iii) The *coding rate* (CR), chosen in the set [4/5, 4/6, 4/7, 4/8], defines the redundancy which can be optionally added to the LoRa messages by employing Forward Error Correction (FEC) codes: the higher the coding rate the higher protection against interference, but the lower the bit rate. (iv) The *transmission power* (P_{tx}) which can be adjusted from -4dBm and +20dBm.

LoRa specifications define region-specific recommended combinations of the aforementioned physical layer parameters which are compliant with the local available spectrum and regulations. As an example, Table I reports the recommended combinations of SF and BW for Europe with the corresponding physical data rate. The proper configuration can be decided at design time and/or changed at run-time using automatic algorithms which are typically run by the network server in a centralized fashion.

At the medium access control level, LoRaWAN operates in a simple star topology with the network server at the center; three classes of end devices are specified

TABLE I
LoRaWAN PHY CONFIGURATION EXAMPLES

| Configuration | PHY bit rate [bit/s] |
|------------------|----------------------|
| SF=12, BW=125kHz | 250 |
| SF=11, BW=125kHz | 440 |
| SF=10, BW=125kHz | 980 |
| SF=9, BW=125kHz | 1760 |
| SF=8, BW=125kHz | 3125 |
| SF=7, BW=125kHz | 5470 |
| SF=7, BW=250kHz | 11000 |
| FSK | 50000 |

“speaking” three different MAC protocols; class A devices transmit in the uplink using a simple ALOHA-based channel access protocol and can only receive downlink data immediately after an uplink transmission. Class B devices can wake up periodically to receive scheduled downlink data traffic. Class C devices listen continuously and are typically mains-powered devices. Class A devices are, at the moment of writing, the ones with the highest diffusion in the market.

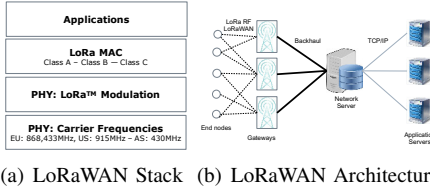


Fig. 1. LoraWAN communication protocol stack (a) and LoraWAN network architecture and components (b).

IV. PROBLEM STATEMENT AND FORMULATION

We address two problems from the perspective of a LoRaWAN network provider: (i) we first consider the case where the LoRaWAN provider is about to roll-out its network and we seek a formal approach to jointly optimize the network layout, the wireless segment and the backhaul links at design time (Section IV-A); then (ii) we assume that the LoRaWAN network operator already has a network in operation (number and positions of the gateways), and we seek a way to optimize the SF assignment and device-to-gateway assignment (Section IV-B). This is a common situation when planning cellular networks where the network layout is planned considering only coverage maximization and then comes the radio resource assignment on the planned network.

A. Joint Planning of Network Layout and Radio Link configuration

Let us define $J = \{1, 2, \dots, M\}$ to be the set of candidate sites indices where LoRaWAN gateways can be deployed and $I = \{1, 2, \dots, N\}$ the set of LoRaWAN end nodes indices to be covered. Sets J and I are generally known by the network provider either through accurate survey of the area to be covered (the former) and through market-driven traffic predictions [20]. It is further convenient to define the set J_i of candidate site

reachable by client i ordered from the closest to the most far away. Depending on the geographical position of the candidate site different backhauling technologies might be available; the set $B_j = \{1, \dots, b_j\}$ includes the available backhauling technologies at candidate site j .

The cost for deploying a gateway at candidate site j and activating there backhauling technology l is defined as c_{jl} with $l \in B_j$. Each backhauling technology is further characterized by an available bandwidth which, in turn, determines a given backhaul transmission delay $t_l^b \in T$, being $T = \{t_1, \dots, t_b\}$ ¹.

Each LoRaWAN end device performs uplink transmissions using one spreading factor in the set $SF = \{1, \dots, 6\}$, which corresponds to the six spreading factor values defined in LoRaWAN specification (see Table I). Each spreading factor induces a transmission delay t_h^a , with $h \in SF$. Let a_{jih} indicate if client i using spreading factor h reaches a gateway at candidate site j . Formally, $a_{jih} = 1$ if an uplink transmission from client i using spreading factor h is received above sensitivity threshold at candidate site j .

The following decision variables are used: $y_{jl} = 1$ if configuration l is activated at candidate site j , $y_{jl} = 0$ otherwise; $z_{ih} = 1$ if user i uses spreading factor h . Let us further define variables x_{ij} to model the assignment of client i to his primary gateway j . Namely, $x_{ij} = 1$ is gateway deployed at candidate site j is the primary gateway for client i .

The problem of minimizing LoraWAN network deployment cost under coverage, latency and data extraction rate constraints can be formalized as follows:

$$\min \sum_{j \in J, k \in B_j} c_{jk} y_{jk} \quad (1)$$

$$\sum_{j \in J} \sum_{l \in B_j} a_{jih} y_{jl} \geq z_{ih} S^* \quad \forall i \in I \quad \forall h \in SF \quad (2)$$

$$\sum_{l \in B_j} y_{jl} \leq 1 \quad \forall j \in J \quad (3)$$

$$\sum_{h \in SF} z_{ih} = 1 \quad \forall i \in I \quad (4)$$

$$e^{-2t_h^* \sum_{i \in I} \lambda_i z_{ih} a_{jih} \sum_{l \in B_j} y_{jl}} \geq \gamma \quad \forall j \in J \quad \forall h \in SF \quad (5)$$

$$\sum_{l \in B_j} y_{jl} + \sum_{s=j+1}^{|J|} x_{is} \leq 1 \quad \forall j \in J_i \quad \forall i \in I \quad (6)$$

$$\sum_{h \in SF} z_{ih} t_h^a + t_l^b \sum_{j \in J} x_{ij} \sum_{l \in B_j} y_{jl} \leq T^* \quad \forall i \in I \quad (7)$$

The objective function (1) tends to minimize the network deployment cost, being c_{jk} the cost for deploying a gateway at candidate site j equipped with backhauling technology k . Constraints (2) enforce each client to be

¹without loss of generality we assume that the packet size used in the uplink is fixed and common to all the LoraWAN clients, so the transmission delay in the backhauling segment depends only on the available bandwidth. No processing delay at the gateways is considered.

able to reach at least S^* gateways; each client then is limited to using one spreading factor by constraints (4) and each gateway is forced to use one backhauling technology by constraints (3).

The set of constraints (5) further enforces that the data extraction rate is at least γ . The constraints builds on the assumption that LoRaWAN medium access control scheme can be well approximated by un-slotted ALOHA as demonstrated in [12] and [16]. The left hand part of the constraints is the expression of the success probability of un-slotted ALOHA when each competing end devices generates Poisson traffic with intensity λ_i and each transmission lasts t_h over the air interface.

Constraints (6) and (7) limit the maximum transmission latency (access delay + backhauling delay) perceived by each end device when using its primary gateway for uplink transmissions. The first term of the constraints ($z_{ih}t_h^a$) represents the over-the-air transmission time, which is summed up with the second term ($t_l^b \sum_{j \in J} x_{ij} \sum_{l \in B_j} y_{jl}$) representing the backhauling transmission delay.

Constraints (6) select as primary gateway for client i the closest deployed one, that is, the gateway which is reached with the highest received power level.

The proposed problem is obviously NP-hard as it contains as sub-problem the Set Covering Problem (SCP). More formally it can be easily proved that any instance of the SCP can be reduced to an instance of the proposed problem with linear transformation. The given formulation which is mixed-integer non linear can be linearized by operating on constraints (5) and (7).

Constraints (5) can be substituted with the following equivalent constraints:

$$\sum_{i \in I} \lambda_i z_{ih} a_{jih} \sum_{l \in B_j} y_{jl} \leq -\frac{\log(\gamma)}{2t_h^*} \quad \forall j \in J \quad \forall h \in SF, \quad (8)$$

which can be linearized as follows:

$$\sum_{i \in I} \lambda_i z_{ih} a_{jih} \leq -\frac{\log(\gamma)}{2t_h^*} + \mathcal{M}(1 - \sum_{l \in B_j} y_{jl}) \quad \forall j \in J \quad \forall h \in SF \quad (9)$$

being \mathcal{M} a quantity that is big enough.

Constraints (7) can be linearized by introducing the variable $k_{il} = x_{ij} \sum_{l \in B_j} y_{jl}$ and substituting the constraints with following ones:

$$k_{il} \leq x_{ij} \quad \forall i \in I \quad \forall j \in J \quad \forall l \in B \quad (10)$$

$$k_{il} \leq \sum_{l \in B_j} y_{jl} \quad \forall i \in I \quad \forall j \in J \quad \forall l \in B \quad (11)$$

$$k_{il} \geq x_{ij} + \sum_{l \in B_j} y_{jl} - 1 \quad \forall i \in I \quad \forall j \in J \quad \forall l \in B \quad (12)$$

B. Stand-alone radio link Configuration

The previously proposed framework can be modified to optimize the radio links of previously planned LoRaWAN networks leading to the following formulation:

$$\max \gamma \quad (13)$$

s.t.

$$\sum_{h \in SF} z_{ih} = 1 \quad \forall i \in I \quad (14)$$

$$e^{-2t_h^* \sum_{i \in I} \lambda_i z_{ih} a_{jih}} \sum_{l \in B_j} y_{jl} \geq \gamma \quad \forall j \in J \quad \forall h \in SF \quad (15)$$

$$\sum_{l \in B_j} y_{jl} + \sum_{s=j+1}^{|J_i|} x_{is} \leq 1 \quad \forall j \in J_i \quad \forall i \in I \quad (16)$$

$$\sum_{h \in SF} z_{ih} t_h^a + t_l^b \sum_{j \in J} x_{ij} \sum_{l \in B_j} y_{jl} \leq T^* \quad \forall i \in I \quad (17)$$

The objective function (13) together with constraints (15) tends to maximize the minimum achievable data extraction rate in the network by properly assigning one spreading factor to each end device (constraints 4). Constraints (16) and (17) are similar to the ones defined in the original formulation in Section IV-A. Constraints (15) and (17) can be easily linearized as shown in Section IV-A. Note that y_{jl} indicating whether configuration l is active at candidate site j are no longer variables but rather parameters in the formulation above.

V. PERFORMANCE EVALUATION

We report here on the performance evaluation of LoRaWAN network layout optimally planned by leveraging the optimization framework introduced in Section IV. As a reference playground, we consider a 5[km] x 5 [km] area of the city of Milan. Different number of candidate sites, M , and LoRaWAN end devices, N , are placed in the reference area; the former are positioned on a grid whereas the latter are randomly drawn in the reference arena. The tests are carried out by using a standard logarithmic path loss model which defines the path loss (in dB) at distance d from the transmitter as:

$$PL(d) = PL(d_0) + 10\alpha \log(d/d_0) + X,$$

where $PL(d_0)$ is the path loss value at a reference distance d_0 , α is the path loss gain and X is a Gaussian variable with zero mean and σ_{shad} standard deviation representing a log-normal path loss component due to shadowing effects. The parameters of the aforementioned model are set in the following experimental campaign according to the setting in [6]. An emitted power level of $P_{tx}=14$ dBm is considered and we assume that an end devices is covered if it reaches a reference gateway with a received power level which is above a sensitivity value, P_{min} ; in our experiments, we used the sensitivity values derived in [12] and reported in Table II.

In the following evaluation, we start off by considering a single option for backhauling technologies for all the deployed gateways; namely, we assume that 3G backhauling is used at all the deployed gateways with a related backhauling transmission rate of 5.7[Mb/s]. The over-the-air transmission time depends on the spreading factor used for transmission; the values used in the

TABLE II
PARAMETER SETTING SUMMARY.

| Parameter | Description | Values |
|-----------------------------|---|---|
| N | number of end devices | [200, 400] |
| M | number of candidate sites | [9, 16, 25] |
| S | minimum number of covering gateways | [3] |
| T^* | maximum transmission delay [ms] | [45 90 170 350 700] |
| γ | maximum Data Extraction Rate | [0.6 0.7 0.75 0.8 0.85] |
| $\lambda_i \forall i \in I$ | message transmission frequency | 0.5 [msg/minute] |
| d_0 | reference distance of propagation model | 1 [km] |
| α | propagation model coefficient | 2.32 |
| P_T | transmitted power | 14 [dBm] |
| σ_{shadow} | standard deviation of lognormal shadowing | 7.8 [dBm] |
| $PL(d_0)$ | path loss at d_0 | 128.95 [dB] |
| P_{min} | sensitivity values at SF 7 thru 12 | [-126.5, -127.25, -131.25, -132.25, -134.5, -135.25] [dB] |

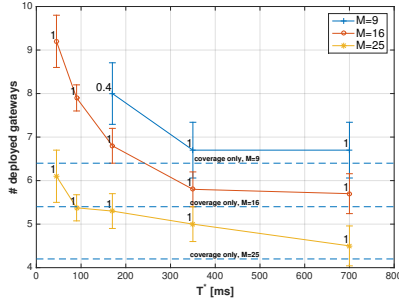


Fig. 2. Number of deployed LoRaWAN gateways versus target values for end-to-end latency for different numbers of available candidate sites (M). $N = 200$. $\gamma = 0.8$

experiments are derived by considering a MAC payload of 26 [byte], a coding rate of 4/5 and a reference bandwidth of 125 [kHz].

Table II describes the parameters involved in the optimization approach and reports the reference corresponding values used in the performance evaluation. It is however worth pointing out that our proposed optimization framework is general and does not depend on the specific assumptions on the propagation model, transmitted power and sensitivity model. In principle, any combination of the three aforementioned factors can be easily plugged in our optimization framework to test different propagation conditions and TX/RX hardware capabilities.

Unless differently stated, the following results were obtained by formalizing the optimization problem of Section IV in AMPL and solving it with CPLEX on a Intel server equipped with two processor Intel Xeon E5620 with four cores each and hyper-threading with 288GB of RAM. The results hereafter report the average over 20 randomly drawn instance of the same type where the position of the candidate sites is fixed whereas the positions of the end devices is randomly drawn in the reference area.

A. Impact of the maximum transmission time

Figure 2 reports the optimal number of deployed LoRaWAN gateways as a function of the maximum allowed transmission delay (T^*) for different values of the available candidate sites (M) in case $N = 200$ end devices need to be covered and the minimum required

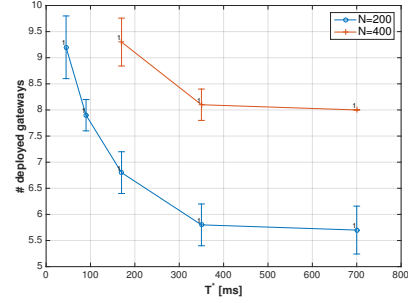


Fig. 3. Number of deployed LoRaWAN gateways versus target values for end-to-end latency for different numbers end devices (N). $M = 16$.

data extraction rate is set to 0.8 ($\gamma = 0.8$). The labels aside each point of the solid lines report the fraction of network instances that were actually, that is, '0.4' means that 60% of the instances were infeasible for the problem at hand.

The dashed lines labelled as "only coverage" report as a benchmark the average number of LoRaWAN gateways deployed when the network layout is planned/optimized under coverage constraints only, that is minimizing the network deployment cost, objective function defined in Eq. (1), subject to constraints in Eqs. (2) only without any constraints on transmission delay and data extraction rate.

Expectedly, the number of deployed gateways decreases when loosening the constraint on the allowed transmission time and when increasing the number of candidate sites as more options are available to the solver. Notably, there is not much difference in the number of gateways deployed by the proposed approach and the benchmark solution obtained when only 3-coverage is enforced; this means that the proposed approach is able to design networks with guaranteed maximum transmission delay and minimum data extraction rate with very minimal budget increase with respect to the 'coverage only' baseline. As an example, looking at the curve referring to $M = 25$, only two more gateways are needed (on average) to guarantee a maximum transmission delay of 45[ms] and a minimum data extraction rate of 0.8.

B. Impact of end devices number

Figure 3 reports the optimal number of deployed LoRaWAN gateways when increasing the number of end devices to be covered to $N = 400$ in the very same settings as Figure 2 ($\gamma = 0.8$). Expectedly, a higher number of gateways is needed when the end devices increase in number. Moreover, as the number of end devices increases, it is no longer possible to guarantee the low values of maximum transmission delays and all the network instances with $T^*=45$ [ms] and $T^*=90$ [ms] are declared non feasible by the solver.

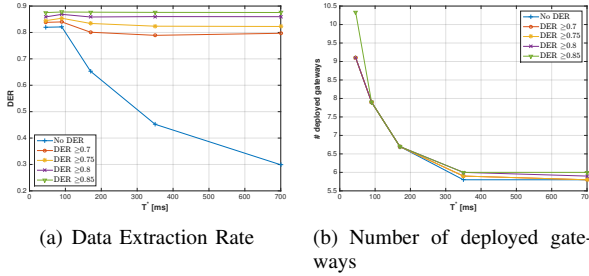


Fig. 4. Data extraction rate and number of deployed gateways for different target maximum transmission delay and different minimum required data extraction rate values. $M = 16$.

Table III report the solution time to get the optimal deployment layout in the same setting as figures 2 and 3. Cells of the table with *NA* indicate that the corresponding instances are not feasible, whereas those cells corresponding to only partial feasibility are indicated with * and the corresponding fraction of feasible instances². Expectedly, the solution time increases exponentially as the network “size” scales up (number of end devices, N , and number of candidate sites, M). Moreover, the solution time also increases when the constraints on the maximum allowed transmission delay gets more loose (higher values of T^*), since the solution space becomes larger.

C. Impact of minimum data extraction rate constraints

It is worth analyzing the impact on the quality of the planned networks of the constraints on the data extraction rate (Eq. 5). To this extent, Figure 4 reports the number of deployed gateways and the average data extraction rate for different target maximum transmission time when changing the minimum required data extraction rate. The curve labelled *No DER* refers to the case in which the network is planned with constraints on the maximum transmission time but without the constraints on the minimum data extraction rate, that is minimizing the objective function defined in Eq. (1), subject to constraints in Eqs. (2), (3) (6), (7).

It can be observed that not considering the constraints on data extraction rate at design phase may lead to network layouts with poor quality down to 0.3 of average data extraction rate (Fig. 4.a) with a negligible reduction of the number of deployed gateways (Fig. 4.b).

D. Joint vs Decoupled Planning

Hereafter, we aim at assessing the performance of the proposed joint planning approach against a good practice adopted in planning classical cellular networks, that is, decoupling coverage planning and radio resource allocation. In the latter case, named *decoupled planning*, we first optimize number and positions of the gateways

²as an example, $274.4^*/0.4$ means that 40% of the network instances were solved getting to an average solution time of 274.4[s].

by considering coverage constraints only under fixed spreading factor assignment (from $SF=7$ to $SF=12$), then, we feed the planned network layout into the model introduced in Section IV-B to optimally assign the spreading factors to maximize the data extraction rate.

Figure 5 reports the comparison between the *decoupled planning* and the *joint planning* approaches. In particular, Figure 5.a shows the data extraction rate obtained when applying the two approaches for different values of maximum allowed transmission delay (T^*), whereas Figure 5.b reports the corresponding number of deployed gateways. Finally, Figure 5.c summarizes the results by plotting the gain in the data extraction rate against the increase in the deployment CAPEX, that is, the difference between the number of deployed gateways when under *joint planning* and under *decoupled planning*.

Notably, the *joint planning* of network layout and radio links leads to network configurations with higher values of data extraction rate at the expense of a almost negligible increase in the number of deployed gateways.

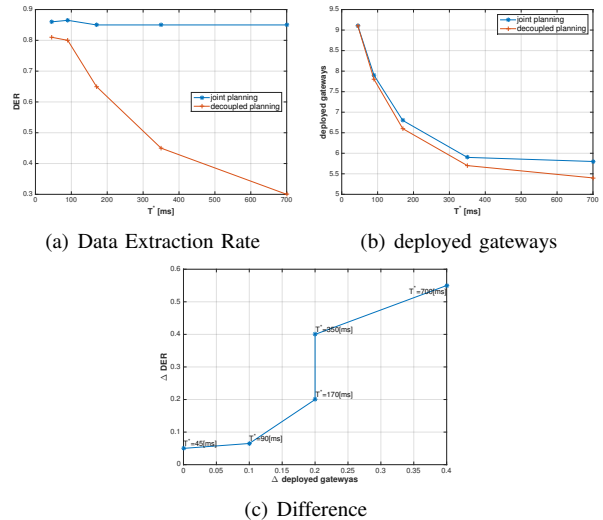


Fig. 5. Difference of number of deployed gateway and data extraction rate when joint and decoupled planning are used. $M = 16$.

VI. CONCLUDING REMARKS

We introduced a mathematical programming framework to design LoRaWAN networks. The proposed approach jointly optimizes at design time the network layout (gateway positions) and the LoRaWAN wireless links (spreading factor assignment) with guaranteed performance in terms of end-to-end uplink transmission time and data extraction rate. We applied the proposed approach to plan LoRaWAN networks in urban environments with the following main take-away messages: (i)

TABLE III
AVERAGE SOLUTION TIME.

| | $T^*=45$ [ms] | | $T^*=90$ [ms] | | $T^*=170$ [ms] | | $T^*=350$ [ms] | | $T^*=700$ [ms] | |
|------|---------------|-------|---------------|------------|----------------|------------|----------------|--------|----------------|---------|
| | N=200 | N=400 | N=200 | N=400 | N=200 | N=400 | N=200 | N=400 | N=200 | N=400 |
| M=9 | NA | NA | NA | NA | 274.4*/0.4 | 411.5*/0.2 | 894.3 | 1306.3 | 4252.43 | 8087.3 |
| M=16 | 15.75 | NA | 70.1 | 119.6*/0.8 | 401.4 | 893.1 | 996.76 | 2087.2 | 6454.4 | 11087.2 |
| M=25 | 36.75 | 89.5 | 75.45 | 201.3 | 467.4 | 998.2 | 1023.5 | 7694.2 | 7987.4 | 15098.4 |

the proposed approach leads to “better” networks with respect to the case where only coverage (network layout) is considered at design phase with negligible increase in the CAPEX; (ii) conversely, the common practice to plan cellular networks decoupling coverage (at planning phase) and radio resource allocation (at operation phase) may lead, in case of LoRaWAN, to extremely poor network performance in terms of data extraction rate.

The proposed optimization framework can be naturally extended in different directions: (i) the transmission of acknowledgedgements in the downlink segment does interfere with the uplink transmissions happening with the same configuration (spreading factor and bandwidth); to this extent, the proposed model can be extended to consider the downlink wireless segment in the formulation of the constraints on the data extraction rate; (ii) although *Class A* devices are still dominant nowadays, LoRaWAN does support for *Class B* and *Class C* devices with superior capabilities in terms of downlink wireless segment; the proposed framework can be extended to include mixed classes of LoRaWAN devices; (iii) the underlying assumption used in the proposed model is that different transmissions collide only if happening in the same bandwidth and with the same spreading factor; some studies demonstrate that the spreading factors used in LoRaWAN are not completely orthogonal, thus opening up for collisions among transmissions with different spreading factors; the proposed model can be easily extended to represent such partial orthogonality among transmissions happening with different spreading factors. Finally, while this work focuses on the modeling aspects of the LoRaWAN optimization, effective heuristics are needed to be able to scale up the size of the planned networks.

REFERENCES

- [1] “Sigfox technology overview,” <https://www.sigfox.com/>.
- [2] “Lora alliance technology,” <https://www.lora-alliance.org/>.
- [3] “Weightless lpwa,” <http://www.weightless.org/>.
- [4] “Ingenu,” <https://www.ingenu.com>.
- [5] M. Aref and A. Sikora, “Free space range measurements with semtech lora technology,” in *2014 2nd International Symposium on Wireless Systems within the Conferences on Intelligent Data Acquisition and Advanced Computing Systems*, Sept 2014, pp. 19–23.
- [6] J. Petajajarvi, K. Mikhaylov, A. Roivainen, T. Hanninen, and M. Pettissalo, “On the coverage of lpwans: range evaluation and channel attenuation model for lora technology,” in *2015 14th International Conference on ITS Telecommunications (ITST)*, Dec 2015, pp. 55–59.
- [7] J. Petajajarvi, K. Mikhaylov, M. Pettissalo, and J. I. J. Janhunen, “Performance of a low-power wide-area network based on lora technology: Doppler robustness, scalability, and coverage,” *International Journal of Distributed Sensor Networks*, vol. 13, no. 3, pp. 55–59, March 2017.
- [8] M. Cattani, C. A. Boano, and K. Rmer, “An experimental evaluation of the reliability of lora long-range low-power wireless communication,” *Journal of Sensor and Actuator Networks*, vol. 6, no. 2, 2017.
- [9] K. Mikhaylov, J. Petijrvi, and J. Janhunen, “On lorawan scalability: Empirical evaluation of susceptibility to inter-network interference,” in *2017 European Conference on Networks and Communications (EuCNC)*, June 2017, pp. 1–6.
- [10] J. Petijrvi, K. Mikhaylov, M. Hmlinen, and J. Iinatti, “Evaluation of lora lpwan technology for remote health and wellbeing monitoring,” in *2016 10th International Symposium on Medical Information and Communication Technology (ISMICT)*, March 2016, pp. 1–5.
- [11] K. Mikhaylov, J. Petijrvi, J. Haapola, and A. Pouttu, “D2d communications in lorawan low power wide area network: From idea to empirical validation,” in *2017 IEEE International Conference on Communications Workshops (ICC Workshops)*, May 2017, pp. 737–742.
- [12] M. C. Bor, U. Roedig, T. Voigt, and J. M. Alonso, “Do lora low-power wide-area networks scale?” in *Proceedings of the 19th ACM International Conference on Modeling, Analysis and Simulation of Wireless and Mobile Systems*, ser. MSWiM ’16. New York, NY, USA: ACM, 2016, pp. 59–67.
- [13] T. Voigt, M. Bor, U. Roedig, and J. Alonso, “Mitigating inter-network interference in lora networks,” in *Proceedings of the 2017 International Conference on Embedded Wireless Systems and Networks*, ser. EWSN ’17. USA: Junction Publishing, 2017, pp. 323–328.
- [14] A. Pop, U. Raza, P. Kulkarni, and M. Sooriyabandara, “Does bidirectional traffic do more harm than good in lorawan based LPWA networks?” *CoRR*, vol. abs/1704.04174, 2017.
- [15] J. Haxhibeqiri, F. Van den Abeele, I. Moerman, and J. Hoebeke, “Lora scalability: A simulation model based on interference measurements,” *Sensors*, vol. 17, no. 6, 2017.
- [16] F. Adelantado, X. Vilajosana, P. Tuset-Peiro, B. Martinez, J. Melia-Segui, and T. Watteyne, “Understanding the limits of lorawan,” *IEEE Communications Magazine*, vol. 55, no. 9, pp. 34–40, 2017.
- [17] O. Georgiou and U. Raza, “Low power wide area network analysis: Can lora scale?” *IEEE Wireless Communications Letters*, vol. 6, no. 2, pp. 162–165, April 2017.
- [18] D.-Y. Kim, S. Kim, H. Hassan, and J. H. Park, “Adaptive data rate control in low power wide area networks for long range iot services,” *Journal of Computational Science*, vol. 22, no. Supplement C, pp. 171 – 178, 2017.
- [19] P. J. Marcelis, V. S. Rao, and R. V. Prasad, “Dare: Data recovery through application layer coding for lorawan,” in *2017 IEEE/ACM Second International Conference on Internet-of-Things Design and Implementation (IoTDI)*, April 2017, pp. 97–108.
- [20] K. Tutschku and P. Tran-Gia, “Spatial traffic estimation and characterization for mobile communication network design,” *IEEE Journal on Selected Areas in Communications*, vol. 16, no. 5, pp. 804–811, Jun 1998.